N-6

HIGH POWER, LOW PHASE DISTORTION, ELECTRONIC FERRITE ATTENUATOR*

L. Dubrowsky, J. Cohen, G. Kern, W. Milberger, R. Porter, J. VanDamme**
Westinghouse Electric Corporation
Baltimore, Maryland 21203

Abstract

This paper discusses the unique design and fabrication methods for the waveguide, coolant channels, and drive yokes of an electronically driven, S-band, high power, four-port, differential phase shift type attenuator. These methods result in a fast-switching, low drive power, low-loss device, with relatively small size and light weight.

Introduction

In some advanced high power transmitter applications, it is necessary to dynamically control output peak power with a low insertion loss device whose insertion phase variation with attenuation is very low. While controlling the output power of a transmitter at low RF drive levels would at first appear to be an advantage, this approach can impose severe constraints on the properties and tolerances of subsequent RF devices in the transmitter chain, resulting in a negative impact on the yield of expensive components. The availability of a high peak and average power attenuator with low loss, low phase distortion, and fast switching allows all the elements of the transmitter chain to operate close to their optimum efficiency and maximum stability points.

Attenuator Description

The attenuator, shown schematically in Figure 1 consists of a folded hybrid tee, two ferrite phasers, and a short slot hybrid. The tee divides the incident RF power in half. The two halves have the the same relative phase as well as the same amplitude. Each divided signal than passes through a phase shift section (ϕ_A, ϕ_B) where a relative phase change is introduced. These signals are then recombined in a short slot hybrid coupler before exiting at the RF output of the attenuator.

A signal passing through phase shifter ϕ_B to the output exhibits a phase lag of 90° relative to ϕ_A due to the coupling coefficients of the short slot coupler. In order to maximize the RF output, the relative phase of ϕ_B to ϕ_A should lead by 90°, permitting both signals to add in phase at the output. Similarly to provide maximum attenuation, the phase of ϕ_B relative to ϕ_A should lag by 90°. In this case the signals flowing in the two paths will cancel at the output.

At the minimum attenuation point, as shown in Figure 2, signal A and B combine in phase with the relative phase of ϕ_B leading that of ϕ_A by 90°. If the phase shifters ϕ_A and ϕ_B are varied in a symmetrical manner, by a phase change δ, so that they approach each other yielding signals which have relative phases:

$\phi_{A'} = \phi_A + \delta$ and $\phi_{B'} = \phi_B - \delta$

Then the output RF signal can be expressed as:

$$RF_{out} = 1/2\, e^{j(\phi_A + \delta)} + 1/2\, e^{j(\phi_B - 90 - \delta)}$$

But $\phi_A = 0°, \phi_B = 90°$

Thus $RF_{out} = 1/2\,(e^{j\delta} + e^{-j\delta})$

$RF_{out} = \cos\delta$

and $RF_{out}(dB) = 20 \log_{10} (\cos \delta)$

Thus it is seen that the vector sum of the attenuated signal theoretically has the same phase for symmetrical phase changes of δ, as that of the unattenuated signal and that the attenuation function is simply the logarithm of a cosine function.

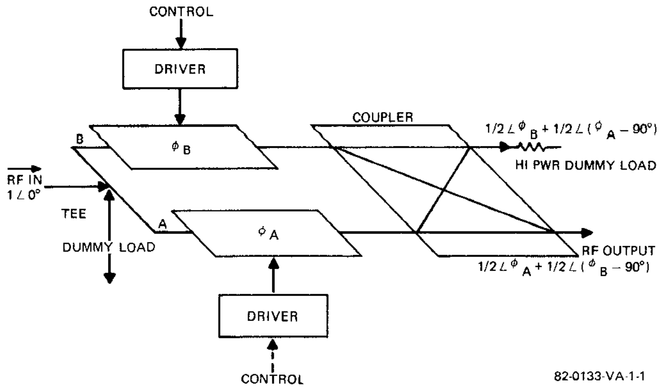

Figure 1. Attenuator Schematic

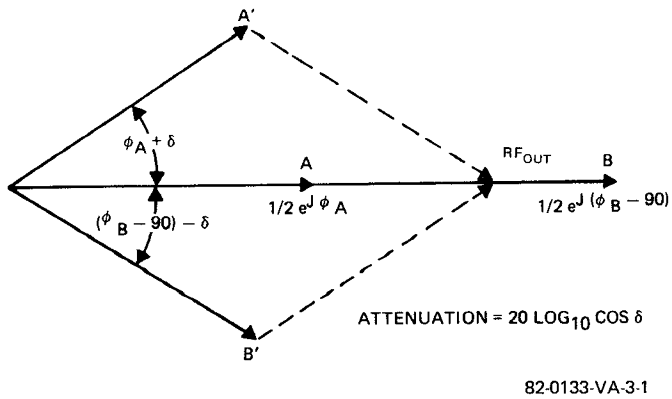

Figure 2. Signal Recombination

Phaser Fabrication

The attenuation and consequently the phase shift sections of the attenuator are required to switch rapidly. This is accomplished by changing the direction between the maximum magnetic fields passing transverse to the waveguide. This fast switching requirement means that the waveguide material must be highly resistive, and that metal thicknesses need to be kept as thin as possible in order to minimize the induced eddy currents.

In conflict with the requirement that the waveguide walls be thin and highly electrically resistive, the high RF power flow in the waveguide requires that the internal walls be good conductors, electrically and thermally, to minimize insertion losses and the subsequent additional variation in thermal load with applied RF power. In addition, the phase shift structure is large, and is required to have good mechanical integrity.

In order to reduce eddy currents in the waveguide, 0.035 inch thick stainless steel, because of its high resistivity, was selected as the wave-

* This work was supported by the Rome Air Development Center, Griffiss, AFB., 13441, NY under contract F30602-81-C-0057
** Mr. Van Damme is with the Rome Air Development Center

guide structural material. A thin internal copper plate is then employed as the RF conductor providing an optimum combination of materials for fast switching, low insertion loss, and mechanical integrity.

The construction of the stainless steel waveguide is shown in Figure 3. Initially, half waveguide sections are built. These are vacuum-furnace brazed assemblies made from four basic parts; the "u" channels which form the actual waveguide, the frame and cover which form the coolant passage, the lanced fins inside the coolant passage, which provide both enhanced heat transfer to the fluid and structural rigidity for the entire assembly, and the coolant fittings.

After furnace brazing these parts, the half waveguide assemblies are copper plated and gold flashed on the inside and the ferrite is bonded in place. The two halves are then joined by laser welding and the flanges are laser welded to the assembly. The flanges are machined smooth and square with the waveguide and the weld seams and flanges are brush plated with copper and gold. This makes a complete waveguide assembly 26.25 inches long.

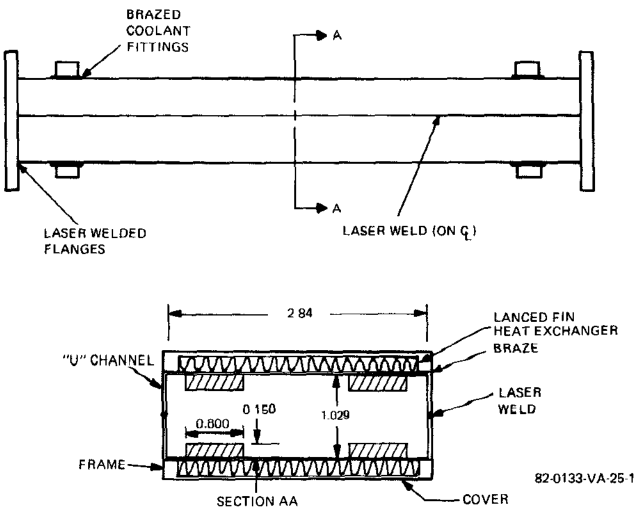

Figure 3. Configuration

Electromagnet Design

The electromagnet design was configured as shown in Figure 4. Silicon steel laminations 0.014 inches thick initially comprised one hundred percent of the yoke material. This configuration weighed close to 200 pounds and required two kilowatts of holding power to produce maximum or minimum attenuation.

The reluctance of the leakage path across the yoke legs (ℓ_ℓ) was less than the reluctance across the waveguide path. (ℓg), and acted as a partial magnetic short. As a result, excessive current and power was required to obtain the desired 400 gauss field across the waveguide.

A determination was made that the gap reluctance was five hundred times greater than the magnet metal path reluctance. Reducing this reluctance ratio to one hundred by replacing 83 percent of the the steel laminations with nonmagnetic transformer pressboard led to several improvements. First, the reluctance of the leakage path was substantially increased. Second the weight of the drive yoke was reduced by 62 percent. Finally the inductance was reduced by 20 percent. These benefits contributed to a final holding power of 450 watts, a weight of 72 pounds, and a reduced switching voltage requirement.

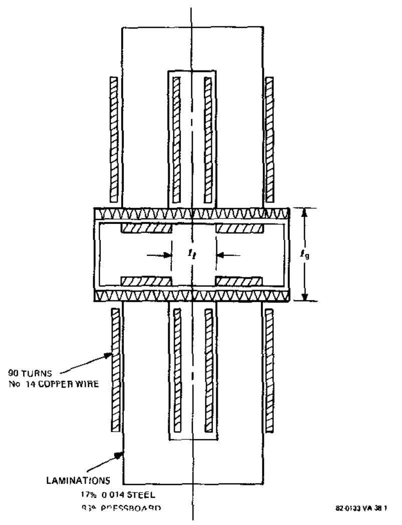

Figure 4. Electromagnet Drive Winding

Microwave Configuration

The microwave configuration, like almost all the other aspects of the design represents compromises between conflicting parameters. The height of the waveguide is reduced from that of standard WR284 waveguide to 1.029 inches. This represents a tradeoff between RF peak power capability and the control power needed to magnetize the air gaps.

Two basic configurations were evaluated at low signal levels. These assemblies are known as the two slab and four slab configurations. The former consists of two rectangular slabs of ferrite, each one mounted on one of the broadwalls of the waveguide. The locations of these slabs is centered one-quarter of the waveguide broadwall dimension in from the same short wall. The latter configuration has four such ferrite slabs, two slabs mounted on each broadwall. This location corresponds to the region of maximum circular polarization of the microwave magnetic field in an empty waveguide. Figure 3 shows the four slab microwave structure that yields optimized microwave performance.

The four slab configuration has the advantage that the RF dissipation is spread out over twice the area in contact with the waveguide than that using an optimum two slab configuration. The thickness of the slabs in the four slab (0.15 inch) configuration is less than that of the two slab configuration (0.2 inch). In addition, the RF dissipation in each slab in the four slab configuration is 30 percent that in the two slab configuration. The net result is that the temperature rise of the ferrite in the four slab configuration is less than 12 percent that in the two slab configuration.

The disadvantage of the four slab configuration is that it requires twice as much ferrite and magnet structure as the two slab. Both of these factors contribute to weight and cost. The fact that the four slab configuration requires more than twice the control power to magnetize the two air gaps at first appears to be a disadvantage. Control power, however, comes at a relatively high efficiency compared to microwave power. The lower insertion loss of the four slab geometry results in a power savings at 80 kW average power of eight times the additional prime control power required, assuming a 90 percent driver efficiency and 40 percent transmitter efficiency.

The material used in this attenuator is twenty inch long slabs of Trans Tech TT2-113 nickel-aluminum ferrite specially selected for low dielectric loss. Empirically optimized figures of merit for the phase shifters were 464 degrees/dB and 763 degrees/dB for the two and four slab configurations respectively.

Phase Variation

The drive coils of both phase shifters were connected in series. Thus the same current will flow through each electromagnet. Applying equal current to both electromagnets does not in a practical device, however, result in equal changes in phase (δ) due to the nonsymmetry of the microwave hysteresis loops. For a given MMF, more rapid phase change is obtained when the phase shifter is driven towards cutoff. The output phase response will thus be the difference between the phase responses of the two hysteresis curves and should be monotonic. As shown in Figure 5 a variation in phase of 7.5 degrees RF was observed over an attenuation range of 40 dB. The deviation from phase linearity over this attenuation range was measured as ± 1.5 degrees RF. This apparent deviation is substantially influenced by the VSWR of the measurement apparatus (1.16/1). This VSWR could result in an error of as much as ± 4.2 degrees RF.

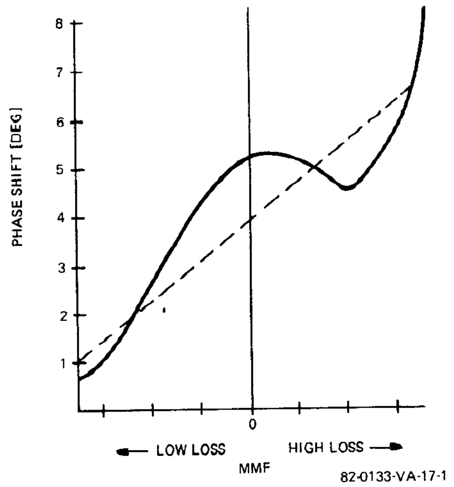

Figure 5. Phase Drive Characteristic

Measured Performance

The VSWR at the output port (1.08 max.) was somewhat better than at the input port (1.2 max.) over the twelve percent band. This is due to the fact that at the input, the in phase reflections from the phase shifters are returned to the source. At the output, the in phase reflections are returned to the terminated port. The insertion loss of the attenuator was measured electrically to be 0.16 dB at low power.

At 1 MW peak, 40 kW average power levels it was determined calorimetrically, by accurately measuring flow rate and inlet and outlet coolant fluid temperatures, that the insertion loss was 0.17 dB. A maximum attenuation of 40 dB could be obtained over any 80 MHz band by adjusting the electromagnet drive. Thirty dB of attenuation could be obtained over an instantaneous twelve percent band. At high power, the output phase variation was less than ± 2.0 degrees over a 27 dB attenuation range.

Calculations, based on calorimetric measurements made at high power, indicated that at 2 MW peak, 80 kW of average power, the mean temperature of the ferrite slabs would be less than 15°C above the inlet coolant temperature.

Drive Power

Measurements and calculations of drive power usage indicated that at 80°C, and 500 μsec switching speed, 2.8 kV at less than 1.5 kW average peak switching power is required. The average power needed to vary the attenuation from 0 to 30 dB at a 100 Hz rate was measured as 221 watts. Finally the maximum holding power at the zero or maximum loss condition was measured as 450 watts. The switching sequence used and power dissipations are shown in Figure 6. The continuous power dissipation is less than 300 watts.

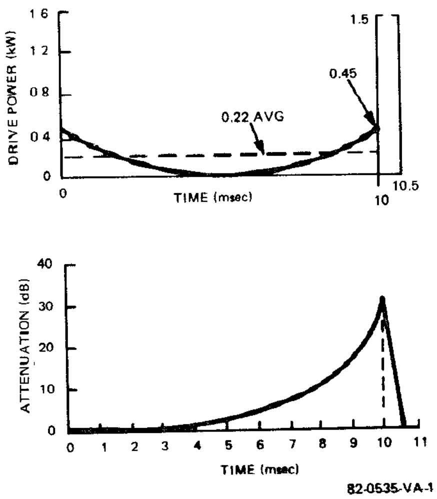

Figure 6. Switching Sequence and Power Distribution

Acknowledgement

The authors are indebted to Mr. Ronald Goodman for his contributions toward the development of the stainless steel waveguide fabrication process.